Med Biol Eng Comput (2017) 55:1085–1096
DOI 10.1007/s11517-016-1562-1

SPECIAL ISSUE – ORIGINAL ARTICLE

Mathematical model of tumor volume dynamics in mice treated with electrochemotherapy

Tadeja Forjanič[1] · **Damijan Miklavčič**[1]

Received: 2 December 2015 / Accepted: 2 September 2016 / Published online: 22 September 2016

Abstract The effectiveness of electrochemotherapy, a local treatment using electric pulses to increase the uptake of chemotherapeutic drug, includes several antitumor mechanisms. In addition to the cytotoxic action of chemotherapeutic drug, treatment outcome also depends on antitumor immune response. In order to assess the contribution of different antitumor mechanisms to the observed treatment outcome, we designed a model of tumor volume dynamics, which is able to quantify early and late treatment effects. Model integrates characteristics of both main posttreatment processes, namely removal of lethally damaged cells from tumor volume and tumor–immune interaction. Fitting to individual responses gives the insight into the dynamics of tumor cell elimination. Two more or less clearly separable peaks can be observed from these dynamics. Model was used to quantify responses obtained after chemotherapy and electrochemotherapy with bleomycin and cisplatin in immunocompetent and immunodeficient mice. As expected, electrochemotherapy resulted in higher number of lethally damaged cells as well as in stronger immune response compared to chemotherapy alone. Additionally, bleomycin-treated tumors proved to be more immunogenic than cisplatin-treated tumors in the given range of doses.

✉ Damijan Miklavčič
damijan.miklavcic@fe.uni-lj.si

Tadeja Forjanič
tadeja.forjanic@fe.uni-lj.si

[1] Department for Biomedical Engineering, Faculty of Electrical Engineering, University of Ljubljana, Trzaska 25, 1000 Ljubljana, Slovenia

Keywords Electroporation · Electrochemotherapy · Mathematical model · Tumor growth

1 Introduction

Electrochemotherapy is a local anticancer treatment achieving an improved chemotherapeutic action by increasing cell membrane permeability [19, 22, 31, 33]. This increased permeability is achieved by local application of short, high-intensity electric pulses which induce changes in cell membrane resulting in transient enhancement of molecular transport across the membrane. Thus, electrochemotherapy relies on electroporation [13], a phenomenon of increased membrane permeability achieved by electric pulses, which enables enhanced uptake of chemotherapeutic drug into the treated cells. Electrochemotherapy is used in daily clinical practice for treatment of primary and metastatic skin tumors. Comparison between different treatments of cutaneous metastasis showed that electrochemotherapy is at least as efficient as other standard treatments (photodynamic therapy, intralesional therapy, topical therapy and radiotherapy) [32]. Moreover, electrochemotherapy is also very effective for the treatment of internal tumors, as confirmed by first clinical experiences [8, 20].

Tumor response to electrochemotherapy should be considered as the result of several mechanisms, contributing to the beneficial treatment outcome. In addition to the chemotherapeutic cytotoxicity, there are at least two mechanisms, affecting final treatment outcome—antivascular action and immune response.

Electrochemotherapy affects the tumor perfusion leading to increased hypoxia levels and extended exposure to chemotherapeutic drug, which remains entrapped in the tumor area [28]. In addition to immediate, but transient

vascular lock, electrochemotherapy also has a prolonged reduction of tumor blood flow due to cytotoxic effect on endothelial cells (vascular disruption action) [11, 17, 28]. The long-term lack of oxygen and nutrients enhances the cell death of surviving cells supplied by the damaged blood vessels. On the other hand, tumor cells in hypoxic environment can become more resistant and can repopulate tumors after chemotherapy and radiotherapy [34]. Increased tumor hypoxia after application of electric pulses was also demonstrated by enhanced antitumor effectiveness of tirapazamine, a hypoxia-activated drug [5].

Additional antitumor mechanism is the immune response, which plays vital role in eradication of surviving tumor cells, thus preventing tumor regrowth. This was confirmed by studies showing that complete responses could only be obtained in immunocompetent mice, whereas in immunodeficient mice only partial responses were achieved [3, 27]. The immune system seems to play important role also in other cancer treatment modalities [1], among others chemotherapy [2, 35] and radiotherapy [10]. Although the exact mechanisms of the so-called immunogenic cell death [15] are not yet fully understood, it is clear that surface exposure and release of certain molecules from dying tumor cells activate the immune cell recruitment [29]. Local immune response was demonstrated also by histological analyses confirming the immune cell infiltration in the tumor area [16].

Evaluation of anticancer treatments, including electrochemotherapy, is often limited to the observation of long-term outcomes [18]. Monitoring the time course of tumor response can, however, provide additional information regarding the treatment effectiveness and enables a more comprehensive comparison between individual responses. Through the development of models describing tumor volume dynamics, we can obtain cell survival fraction or other measures of treatment efficacy. Modeling of the tumor volume dynamics is already extensively used in oncology drug development [23, 25] and in radiotherapy [9, 26].

In human patients, it is often difficult to obtain sufficient information needed for model development due to limited follow-up examinations after electrochemotherapy. However, the results of preclinical studies conducted on animal tumor models are usually presented by daily measurements of tumor size. In this paper, we present a mathematical model describing the dynamics of the number of tumor cells in mice tumor model following electrochemotherapy. Such model enables estimating the contribution of early (direct cell kill) and delayed treatment effect (immune response) on the observed dynamics. Thus, the model can serve as a tool to compare different tumor responses and to better understand the effects of a specific type of the treatment.

2 Methods

2.1 Animal studies

The data used in this study were in detail described in [4, 27, 30]. Subcutaneous SA-1 sarcoma tumors in A/J mice were subjected to a treatment with BLM [4] or CDDP [30] alone or in combination with high-voltage electric pulses. Electrochemotherapy was performed by eight 100-μs electric pulses of 1040 V amplitude and 1 Hz repetition frequency delivered by two plate electrodes separated by 8 mm. This protocol resulted in sufficiently high electric field throughout the tumor so most of the cells were permeabilized [21, 24]. After the day of the treatment (day 0), tumor volume was determined by daily measurements of three mutually orthogonal diameters (e_1, e_2 and e_3) according to the formula: $V = \frac{\pi}{6} e_1 e_2 e_3$. In the third study, [27], LPB sarcoma was treated in immunocompetent C57B1/6 and immunodeficient Swiss *nu/nu* mice. Chemotherapy and electrochemotherapy with different doses of cisplatin were performed on 25 mm^3 tumors using parallel plate electrodes, spaced 6 mm apart. Pulse parameters (8 pulses of 100 μs width and amplitude of 780 V, delivered at 1 Hz) again assured a successful permeabilization of the majority of tumor cells [6]. In all experiments, drug was injected only on day 0 and pulses were delivered 3 min later, which was demonstrated to be the optimal timing for achieving the highest electrochemotherapy effectiveness of BLM [7] as well as CDDP [30].

2.2 Unperturbed growth

In general, after tumor cell inoculation, tumor begins to grow exponentially, and then, the growth slows down to linear rate, eventually reaching a plateau phase. Since only exponential and linear growth phases can be observed in our experimental data, we adopted a function originally proposed by Koch et al. [12] with smooth transition between exponential and linear growth:

$$\frac{\mathrm{d}X}{\mathrm{d}t} = \frac{2\lambda_0\lambda_1 X}{(\lambda_1 + 2\lambda_0 X)} \tag{1}$$

2.3 Tumor response modeling

Tumor volume was converted to the number of tumor cells assuming a cell density of 10^9 cells/cm^3 in order to model tumor–immune interaction. The model consists of four differential equations. At the day of the treatment (day 0), all tumor cells belong to the first compartment (x_1). Tumor cells, damaged by the treatment, move to the second compartment (x_2), where they still contribute to the total tumor volume, but do not divide anymore. Since

dead-cell resolving takes place soon after the treatment, an exponentially decaying function was employed to limit this process to a first few days after the treatment. Tumor cells die, at least partially, in an immunogenic manner, thereby stimulating the recruitment of immune cells (y) [36]. Since we were specifically interested in the treatment-induced immune response, the initial number of immune cells, y_0, is set to 0. In order to account for the time required to stimulate the immune response, we introduced the third compartment in the model. With parameter b, we also enabled some flexibility at the initial phase of immune response. Equation (2d) describes the dynamics of immune cell population, present at the tumor site, y. Since we wanted to keep the model simple, y includes all types of immune cells. Nevertheless, Eq. (2d), based on the model describing the dynamics of immunogenic tumors by Kuznetsov et al. [14], captures all main characteristics of tumor–immune interaction. Treatment-induced immune response is initiated through the process of immunogenic cell death, meaning that parameter c can be interpreted as a measure for immunogenicity of dying tumor cells. Subsequent recruitment of immune cells is modeled by Michaelis–Menten dynamics to include the saturation effect of the immune response. Further, immune-mediated tumor cell killing leads to mutual decrease in both cell populations. Finally, the number of immune cells decreases due to natural death. Hence, complete system of differential equations reads:

$$\frac{\mathrm{d}x_1}{\mathrm{d}t} = \frac{2\lambda_0\lambda_1 x_1^2}{(\lambda_1 + 2\lambda_0 x_1)(x_1 + x_2)} - de^{-kt}x_1 - nx_1y \tag{2a}$$

$$\frac{\mathrm{d}x_2}{\mathrm{d}t} = de^{-kt}x_1 - \mathrm{d}x_2 \tag{2b}$$

$$\frac{\mathrm{d}x_3}{\mathrm{d}t} = \mathrm{d}x_2 - bx_3 \tag{2c}$$

$$\frac{\mathrm{d}y}{\mathrm{d}t} = cx_3 + p\frac{x_1 y}{g + x_1} - mx_1 y - ay, \tag{2d}$$

with initial conditions:

$$x_1(0) = x_{10}, \quad x_2(0) = 0, \quad x_3(0) = 0, \quad y(0) = 0$$

Total number of tumor cells is described by the sum of the first and second compartment:

$$X(t) = x_1(t) + x_2(t) \tag{3}$$

Parameter n describes tumor cell killing by immune cells, whereas m describes the immune cell inactivation as a result of this interaction. Further, parameter p denotes the rate of immune cell recruitment, whereas g denotes the steepness of the recruitment curve. The value for g was taken from the literature ($g = 2.019 \times 10^7$ cells) [14]. In order to distinguish between early and late treatment effect, we limited the death of directly damaged cells to a first few days following the treatment by setting a minimum value of parameter k to 0.2 day^{-1}. Parameters were estimated for each individual response, except for the data of immunodeficiency study, where only average data were available. Estimation of parameters was performed using *fitnlm*, a MATLAB's nonlinear model fitting tool.

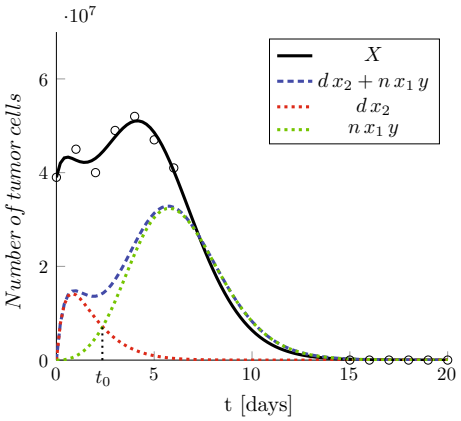

Fig. 1 Complete response with two distinctive peaks, corresponding to dying process of damaged cells ($d\,x_2$) and immune-mediated cell killing ($n\,x_1\,y$)

3 Results

Fitting tumor growth curves to the control group data gave exponential and linear growth rates. Average values were $\lambda_0 = 0.346$ day^{-1} and $\lambda_1 = 1.24 \times 10^8$ cells/day for the mice treated with BLM and $\lambda_0 = 0.357$ day^{-1} and $\lambda_1 = 0.70 \times 10^8$ cells/day for the mice treated with CDDP. From the data of immunodeficiency study, we obtained two linear growth rates: 0.57×10^8 cells/day for immunocompetent mice and 0.62×10^8 cells/day for *nu / nu* mice. However, due to lack of pretreatment growth data, exponential growth rate was fixed to 0.3 day^{-1}.

The proposed model fitted individual responses very well (average $R^2 = 0.992$ for BLM study and average $R^2 = 0.989$ for CDDP study). However, high number of free parameters resulted in high dispersion of parameter estimates (Table 1). Therefore, we estimated a total number of tumor cells, killed directly or by immune mechanisms, as a more valuable and objective measure of treatment efficacy. The contribution of each cell killing mechanism can be assessed from the tumor volume dynamics. By some complete and also partial responses, we can observe two distinctive peaks in a first few days after the treatment (Fig. 1). This dynamics is successfully captured by our model, indicating that first peak corresponds to dying of directly damaged cells and second

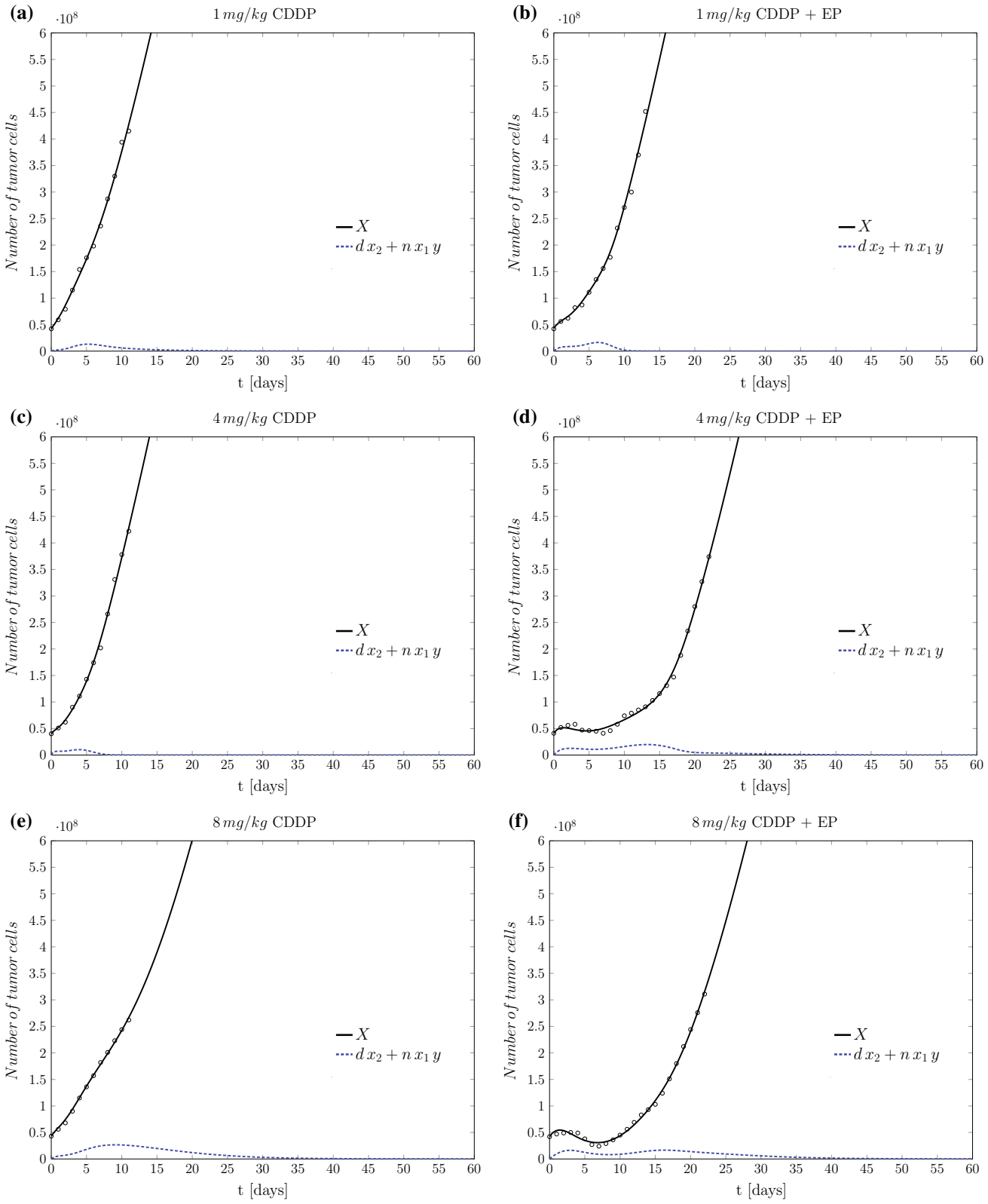

Fig. 2 Selected responses of mice treated with CDDP together with fitted curves. The *left column* shows typical responses obtained after chemotherapy with different doses of CDDP: 1 mg/kg (**a**), 4 mg/kg (**c**) and 8 mg/kg (**e**), whereas the *right column* shows corresponding responses after electrochemotherapy. *Solid line* represents the total number of tumor cells while *dashed line* represents the number of dying tumor cells either due to drug cytotoxicity or immune response

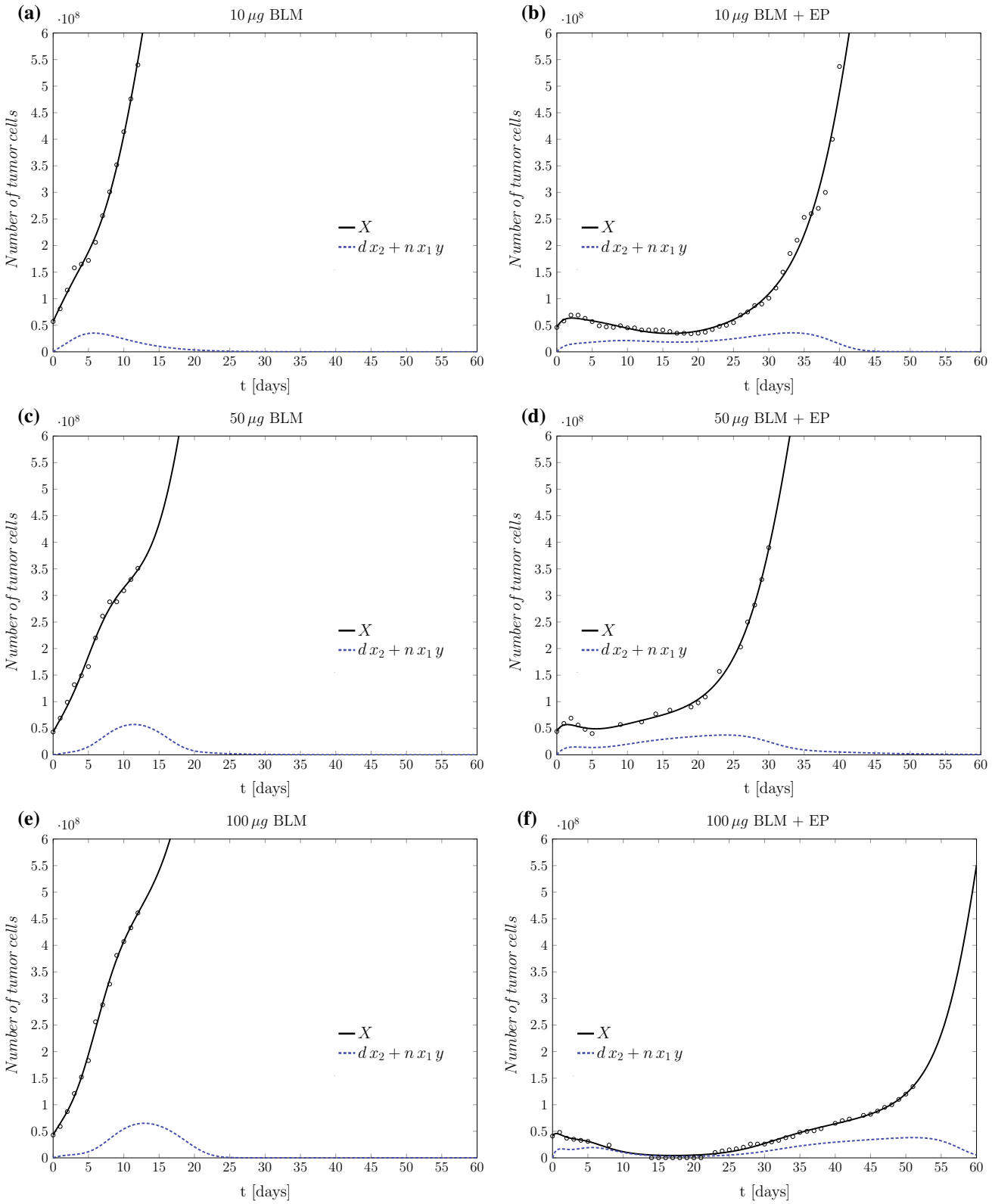

Fig. 3 Selected responses of mice treated with BLM-based chemotherapy and electrochemotherapy together with fitted curves. Similar to Fig. 2, *left column* shows typical responses obtained after chemotherapy and the *right column* shows corresponding responses after electrochemotherapy

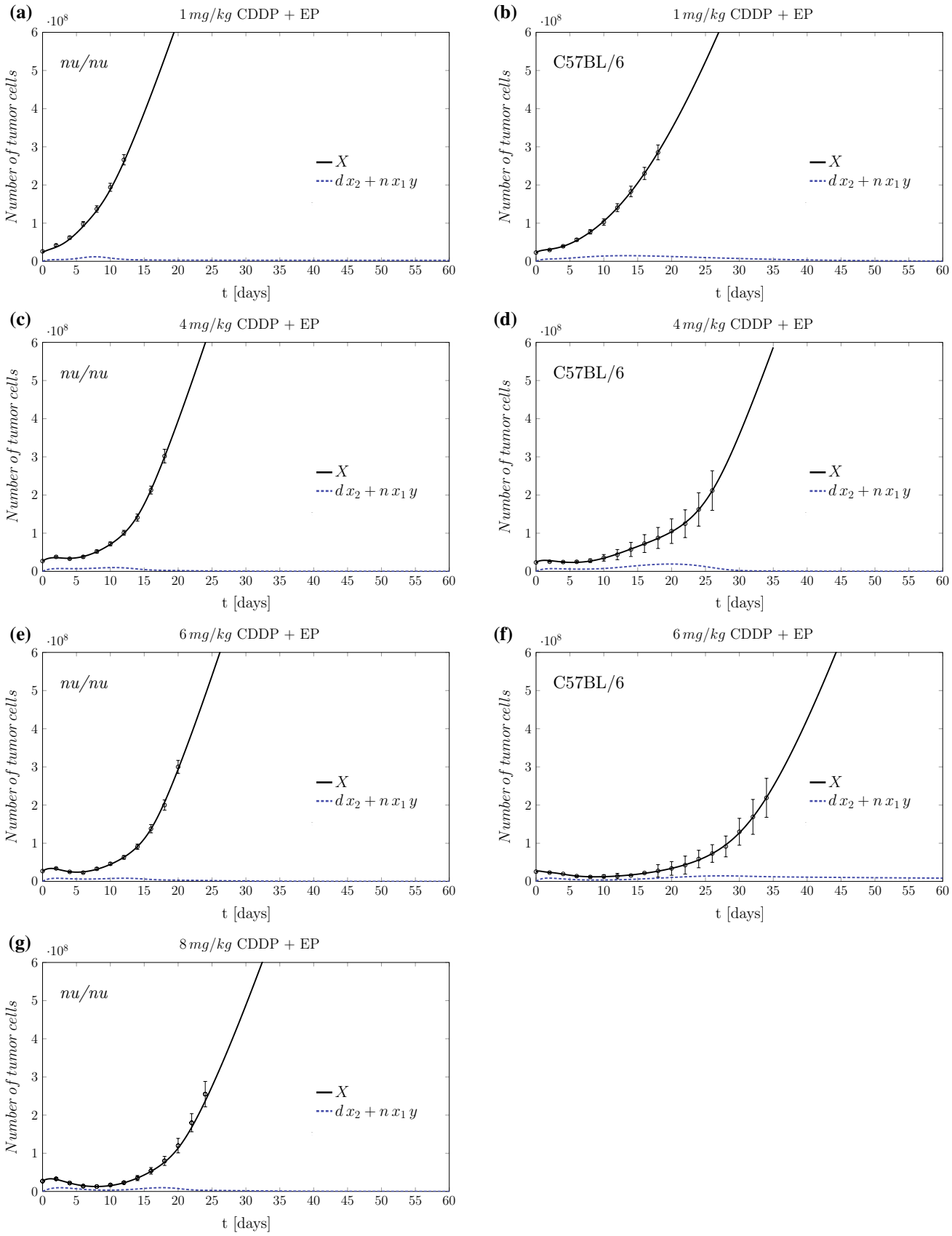
(a)
1 mg/kg CDDP + EP
nu/nu
(b)
1 mg/kg CDDP + EP
C57BL/6
(c)
4 mg/kg CDDP + EP
nu/nu
(d)
4 mg/kg CDDP + EP
C57BL/6
(e)
6 mg/kg CDDP + EP
nu/nu
(f)
6 mg/kg CDDP + EP
C57BL/6
(g)
8 mg/kg CDDP + EP
nu/nu
Number of tumor cells
t [days]
X
d x2 + n x1 y

◂**Fig. 4** Comparison of average responses obtained after CDDP-based electrochemotherapy in immunodeficient *nu/nu* mice (*left column*) and immunocompetent C57B1/6 mice (*right column*). Doses of CDDP used in the study were: 1 mg/kg (**a**, **b**), 4 mg/kg (**c**, **d**), 6 mg/kg (**e**, **f**) and 8 mg/kg (**g**)

peak to immune-mediated cell killing. Moreover, both peaks of cell killing activity are easy distinguishable also in other cases by plotting the time course of killed tumor cells (Figs. 2, 3, 4). Of course, in the cases of weak partial responses peaks become less pronounced, making the separation between both causes of cell death less reliable. In order to objectively separate between both effects, we calculated the time point of equal cell killing efficiency of both antitumor mechanisms according to the model and used it as a limit for integration. More precisely, this time point represented the upper limit for directly killed tumor cells and lower limit for tumor cells killed by immune system.

The calculation of total tumor cell kill is subject to uncertainty arising from the assumption that all animals in each experiment share the same tumor growth parameters.

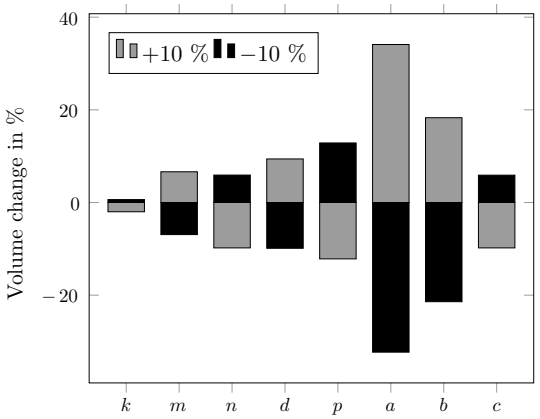

Fig. 6 Percent change in the tumor volume of a selected partial response with 33 days of growth delay after changing each of the parameters for 10 %, one at a time

In order to assess this uncertainty, we first performed the calculation of tumor cell kill on control groups. Average values, obtained from BLM study [4] and CDDP study [30], respectively, were: 0.079×10^8 cells and 0.067×10^8

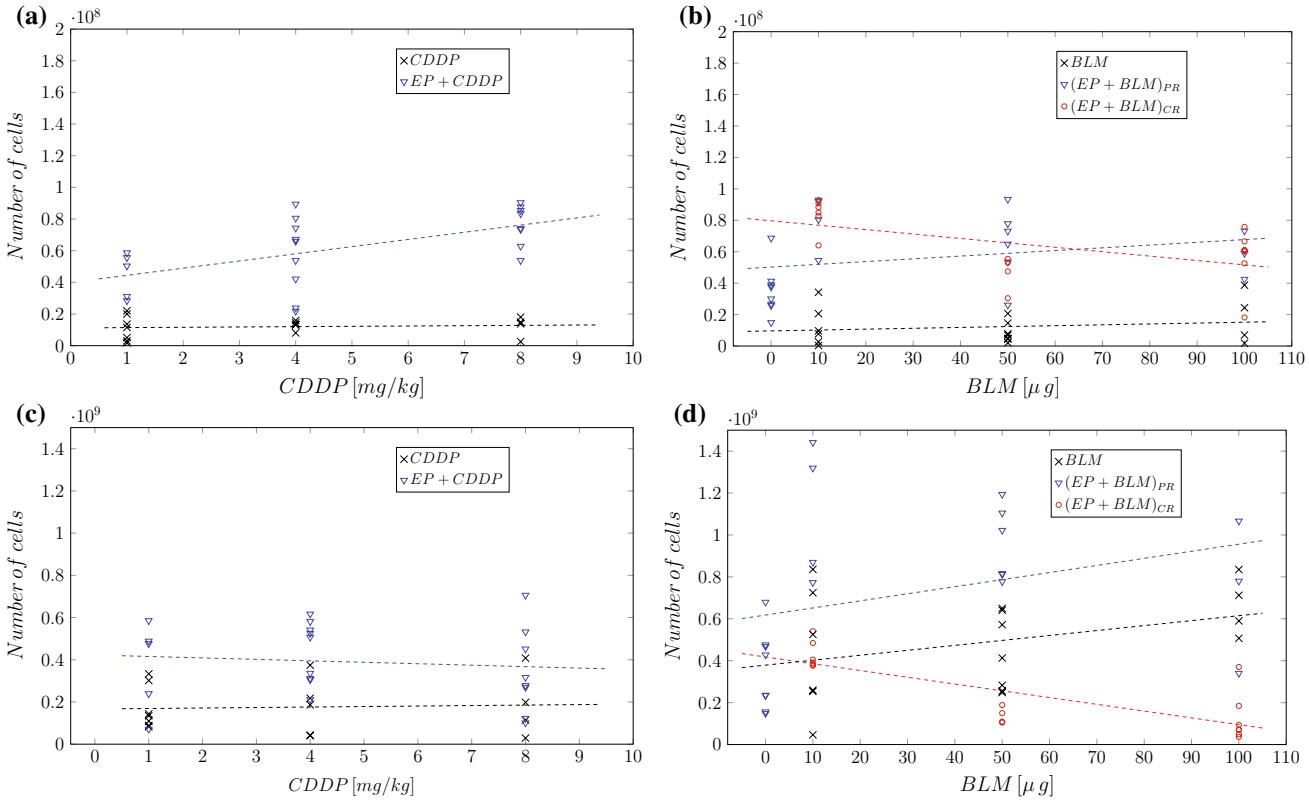

Fig. 5 Number of tumor cells killed directly (**a**, **b**) and number of tumor cells eliminated by immune system (**c**, **d**). Results show that electrochemotherapy effectiveness relies on improved drug action as well as stronger immune response. Complete responses (CR) were achieved only by BLM-based electrochemotherapy, which elicited stronger immune response than CDDP-based electrochemotherapy. Total number of tumor cells killed by immune system is lower by complete responses than partial responses (PR) due to successful elimination of all surviving cells

Table 1 Estimated model parameters obtained by fitting the responses of (a) BLM-treated mice [4] and (b) CDDP-treated mice [30]. Average parameter estimates are given along with their coefficients of variation (between brackets). Additionally, average total number of cells killed due to drug cytotoxicity, $\int_0^{t_0}(dx_2 + nx_1y)\,dt$, and immune activity, $\int_{t_0}^{\infty}(dx_2 + nx_1y)\,dt$, are presented

(a)

Dose [μg]	BLM			EP
	10	50	100	
N	6 PR	5 PR	4 PR	8 PR
k [day^{-1}]	0.576 (46)	0.286 (25)	0.706 (38)	0.618 (50)
m [cells^{-1} day^{-1}]	6.00×10^{-9} (83)	4.61×10^{-9} (75)	1.42×10^{-9} (8)	5.82×10^{-9} (100)
n [cells^{-1} day^{-1}]	4.16×10^{-6}(95)	2.18×10^{-6}(32)	1.38×10^{-6} (74)	1.65×10^{-6} (90)
d [day^{-1}]	0.201 (33)	0.199 (21)	0.253 (36)	0.478 (28)
p [day^{-1}]	0.344 (68)	0.463 (75)	0.519 (46)	0.925 (22)
a [day^{-1}]	0.096 (141)	0.192 (140)	0.078 (162)	8×10^{-5} (120)
b [day^{-1}]	0.337 (78)	0.528 (59)	0.608 (157)	0.686 (61)
c [day^{-1}]	0.0035 (95)	0.0018 (32)	0.0017 (39)	0.0014 (90)
$\int_0^{t_0}(dx_2 + nx_1y)\,dt$	0.13×10^8 (102)	0.09×10^8 (75)	0.18×10^8(94)	0.35×10^8 (45)
$\int_{t_0}^{\infty}(dx_2 + nx_1y)\,dt$	4.41×10^8 (69)	4.37×10^8 (42)	6.61×10^8 (22)	3.53×10^8 (53)

Dose [μg]	BLM + EP					
	10	10	50	50	100	100
N	4 PR	6 CR	6 PR	4 CR	3 PR	7 CR
k [day^{-1}]	0.240 (29)	0.200 (0.2)	0.543 (106)	0.639 (50)	0.416 (60)	0.706 (135)
m [cells^{-1} day^{-1}]	2.44×10^{-9} (76)	8.71×10^{-9} (138)	1.43×10^{-9} (125)	3.56×10^{-9} (138)	1.60×10^{-9} (25)	2.66×10^{-9} (173)
n [cells^{-1} day^{-1}]	1.68×10^{-6} (50)	1.43×10^{-6} (70)	2.16×10^{-6} (38)	2.16×10^{-6} (30)	2.69×10^{-6} (14)	1.67×10^{-6} (106)
d [day^{-1}]	0.575 (2)	0.577 (8)	0.870 (37)	0.952 (14)	0.870 (25)	0.986 (36)
p [day^{-1}]	0.332 (92)	0.177 (94)	0.156 (104)	0.435 (69)	0.293 (49)	1.042 (64)
a [day^{-1}]	0.201 (117)	0.170 (197)	0.091 (82)	0.026 (199)	0.155 (52)	0.0004 (168)
b [day^{-1}]	0.326 (124)	0.071 (245)	0.367 (78)	0.231 (176)	0.382 (35)	0.099 (107)
c [day^{-1}]	0.0014 (50)	0.0012 (70)	0.0018 (38)	0.0018 (30)	0.0022 (14)	0.0014 (106)
$\int_0^{t_0}(dx_2 + nx_1y)\,dt$	0.80×10^8 (22)	0.84×10^8 (12)	0.65×10^8 (36)	0.47×10^8 (24)	0.58×10^8 (26)	0.56×10^8 (32)
$\int_{t_0}^{\infty}(dx_2 + nx_1y)\,dt$	11.01×10^8 (30)	4.29×10^8 (16)	9.54×10^8 (18)	1.38×10^8 (28)	7.29×10^8 (50)	1.25×10^8 (95)

(b)

Dose [mg/kg]	CDDP			CDDP + EP		
	1	4	8	1	4	8
N	7 PR	5 PR	4 PR	5 PR	9 PR	8 PR
k [day^{-1}]	1.893 (38)	2.020 (28)	1.662 (21)	0.681 (76)	0.476 (89)	0.282 (34)
m [cells^{-1} day^{-1}]	2.77×10^{-9} (178)	4.14×10^{-9} (106)	8.95×10^{-9} (89)	10.33×10^{-9} (40)	5.37×10^{-9} (62)	8.78×10^{-9} (50)
n [cells^{-1} day^{-1}]	2.58×10^{-6} (59)	2.34×10^{-6} (37)	4.29×10^{-6} (75)	0.78×10^{-6} (56)	2.15×10^{-6} (70)	2.19×10^{-6} (105)
d [day^{-1}]	0.490 (28)	0.682 (74)	0.634 (40)	0.680 (17)	0.654 (25)	0.730 (16)
p [day^{-1}]	0.161 (145)	0.451 (82)	0.744 (80)	1.502 (12)	0.349 (87)	1.475 (122)
a [day^{-1}]	0.587 (87)	0.270 (119)	0.116 (200)	0.00001 (214)	0.067 (157)	0.806 (176)
b [day^{-1}]	1.52 (52)	0.477 (114)	0.709 (134)	0.309 (129)	0.361 (97)	0.480 (162)
c [day^{-1}]	0.0025 (59)	0.0019 (37)	0.0035 (75)	0.0006 (56)	0.0018 (70)	0.0018 (105)
$\int_0^{t_0}(dx_2 + nx_1y)\,dt$	0.11×10^8 (73)	0.13×10^8 (23)	1.12×10^8 (55)	0.45×10^8 (32)	0.58×10^8 (42)	0.76×10^8 (17)
$\int_{t_0}^{\infty}(dx_2 + nx_1y)\,dt$	1.71×10^8 (61)	1.72×10^8 (81)	1.87×10^8 (87)	3.72×10^8 (32)	4.37×10^8 (33)	3.47×10^8 (59)

N is the number of successfully fitted partial (PR) or complete responses (CR)

Table 2 Results of parameter estimation using the data of study [27], demonstrating the involvement of the immune response in the antitumor effectiveness of CDDP-based electrochemotherapy. Calculated parameter values were used to estimate the contribution of direct and immune-mediated cell kill

(a)

Dose [mg/kg]	Immunocompetent mice (C57B1/6)						
	CDDP			CDDP + EP			EP
	1	4	6	1	4	6	
k [day^{-1}]	0.779	0.771	0.240	0.629	0.217	0.168	3.138
m [cells^{-1} day^{-1}]	8.13×10^{-9}	2.1×10^{-15}	7.1×10^{-12}	1.0×10^{-13}	4.25×10^{-9}	8.91×10^{-9}	0.96×10^{-9}
n [cells^{-1} day^{-1}]	2.76×10^{-6}	3.90×10^{-6}	2.19×10^{-6}	3.89×10^{-6}	1.96×10^{-6}	1.54×10^{-6}	5.94×10^{-6}
d [day^{-1}]	0.653	0.702	0.462	0.622	0.622	0.720	1.137
p [day^{-1}]	0.115	0.562	0.518	0.562	0.943	0.541	0.002
a [day^{-1}]	0.162	0.668	0.717	0.670	0.501	0.387	0.273
b [day^{-1}]	0.116	0.484	1.230	0.7054	0.4539	0.0141	0.273
c [day^{-1}]	0.0023	0.0032	0.0018	0.0032	0.0016	0.0013	0.0049
$\int_0^{t_0}(dx_2 + nx_1y)\,dt$	0.17×10^8	0.16×10^8	0.58×10^8	0.19×10^8	0.47×10^8	0.49×10^8	0.07×10^8
$\int_{t_0}^{\infty}(dx_2 + nx_1y)\,dt$	1.37×10^8	3.76×10^8	3.02×10^8	3.44×10^8	2.85×10^8	4.53×10^8	1.57×10^8
TGD [days]	1.4	2.1	2.2	2.3	16.5	21.4	0.8

(b)

Dose [mg/kg]	Immunodeficient mice (*nu/nu*)				EP
	CDDP				
	1	4	6	8	
k [day^{-1}]	0.772	1.007	0.616	0.502	3.692
m [cells^{-1} day^{-1}]	9.34×10^{-9}	7.68×10^{-9}	9.62×10^{-9}	7.32×10^{-9}	1×10^{-14}
n [cells^{-1} day^{-1}]	1.90×10^{-6}	6.32×10^{-6}	1.53×10^{-6}	0.95×10^{-6}	5.55×10^{-6}
d [day^{-1}]	0.385	0.486	0.450	0.393	1.075
p [day^{-1}]	1.340	2.166	1.414	1.213	0.031
a [day^{-1}]	7.3×10^{-6}	1.157	7×10^{-7}	0.295	0.468
b [day^{-1}]	1.88	3.83	2.11	4.4×10^{-6}	0.554
c [day^{-1}]	0.0016	0.0052	0.0013	0.0008	0.0046
$\int_0^{t_0}(dx_2 + nx_1y)\,dt$	0.12×10^8	0.10×10^8	0.19×10^8	0.21×10^8	0.06×10^8
$\int_{t_0}^{\infty}(dx_2 + nx_1y)\,dt$	0.47×10^8	0.67×10^8	0.75×10^8	1.45×10^8	0.90×10^8
TGD [days]	0.1	0.5	0.7	0.6	0.5

Dose [mg/kg]	Immunodeficient mice (*nu/nu*)			
	CDDP + EP			
	1	4	6	8
k [day^{-1}]	0.732	0.263	0.224	0.200
m [cells^{-1} day^{-1}]	11.38×10^{-9}	10.47×10^{-9}	11.30×10^{-9}	13.26×10^{-9}
n [cells^{-1} day^{-1}]	1.22×10^{-6}	1.29×10^{-6}	1.32×10^{-6}	5.64×10^{-6}
d [day^{-1}]	0.508	0.580	0.650	0.581
p [day^{-1}]	1.248	0.562	0.393	1.571
a [day^{-1}]	0.100	1×10^{-4}	1×10^{-4}	0.619
b [day^{-1}]	3.8×10^{-6}	0.40	0.33	13.71
c [day^{-1}]	0.0010	0.0011	0.0011	0.0032
$\int_0^{t_0}(dx_2 + nx_1y)\,dt$	0.17×10^8	0.49×10^8	0.54×10^8	0.54×10^8
$\int_{t_0}^{\infty}(dx_2 + nx_1y)\,dt$	1.14×10^8	0.93×10^8	1.02×10^8	1.25×10^8
TGD [days]	0.8	5.8	8.4	13.2

cells, killed directly, and 0.659×10^8 cells and $0.723 \cdot 10^8$ cells, killed by immune system.

Keeping these uncertainties in mind, we proceeded to the calculation of tumor cell kill in treated animals. As expected, electrochemotherapy achieved higher number of tumor cells killed directly as well as higher number of tumor cells killed by immune system than chemotherapy. Moreover, both drugs show similar cell killing efficiency over the range of doses used in experiments. However, there are substantial differences in immune response. BLM-based electrochemotherapy elicited substantially stronger immune response compared to CDDP-based electrochemotherapy (Fig. 5). Complete responses resulted in lower number of tumor cells killed by immune system due to successful elimination of all surviving cells. A key role of immune response is further confirmed by results of immunodeficiency study. Nude mice, lacking T lymphocytes, show significantly weaker immune response compared to immunocompetent mice, explaining the difference in tumor growth delays (Table 2).

Due to high number of free parameters, we considered simplifying the model by combining first two compartments or by eliminating certain parameters. Simplified models were compared to the original model using Akaike information criterion (AIC) and Bayesian information criterion (BIC). In most cases, certain simplifications (elimination of the third compartment and $b = d$) turned out to be justified (data not shown). However, these simplified models could not follow the dynamics of highly responsive tumors to BLM-based electrochemotherapy and were therefore excluded from further analysis and discussion.

3.1 Sensitivity analysis

The impact of individual model parameters on the number of tumor cells at day 40 was evaluated by modifying parameter values for 10 % (Fig. 6). Initial parameter values were taken from a case showing partial response from the group of mice treated with BLM-based electrochemotherapy.

4 Discussion

A high variability of tumor responses can be observed not only between different treatment groups, but also within the same group, particularly in the case of BLM-based electrochemotherapy. This variability is visible in terms of differences in tumor growth delays as well as in differences regarding the shape of tumor volume dynamics. Having in mind presumably different mechanisms of immune response depending on the type of the treatment, we had to design a flexible model, able to follow the individual response curves. On the other hand, model had to be robust enough to allow a reliable estimation of direct and immune-mediated cell killing. While the robustness was achieved by following the characteristics of both cell killing mechanisms, flexibility was added by additional compartment, allowing for the differences at the initiation of immune response.

Results are in agreement with existing knowledge that treatment outcome depends on drug cytotoxicity as well as immune response. Mice treated with CDDP-based electrochemotherapy showed only limited level of immune response, and no complete responses were obtained in given range of doses. On the other hand, BLM-based electrochemotherapy induced more potent antitumor immune responses, which again proved to be the key factor for obtaining complete responses. A decrease in number of killed tumor cells with increasing dose observed by complete responses can be explained by faster regression of tumors and thus lower number of surviving cells that have to be eliminated. Interestingly, also tumors treated by electric pulses only showed a weak immune response, comparable to low-dose chemotherapy.

More important than each cell killing mechanism by itself, is their cooperative action. Electrochemotherapy-treated tumors induce a certain level of immune response, which is capable to control a limited number of tumor cells. Therefore, in addition to efficient direct cell kill, it is important that immune response is initiated fast to eliminate surviving tumor cells. Namely, during the time required for immune cell recruitment, surviving tumor cells continue to proliferate, thus enhancing the possibilities to escape from immune control.

Using a single model to analyze such a wide range of tumor responses leads to poor parameter identifiability by weak tumor responses. Nevertheless, estimated parameters related to tumor–immune competition agree well with the values reported in Kuznetsov et al. [14] ($m = 3.422 \times 10^{-10}$ cells^{-1} day^{-1}, $n = 1.101 \times 10^{-7}$ cells^{-1} day^{-1}, $p = 0.1245\,\text{day}^{-1}$, $d = 0.0412\,\text{day}^{-1}$). It is important to keep in mind, however, that we developed our model to reveal the dynamics of treatment-induced tumor cell killing rather than describe the exact mechanisms involved in the tumor response. For improving the identifiability of model parameters, further experiments about the types and the dynamics of immune cells involved are needed. Our work should therefore be seen as the first step toward assessing drug-, treatment- and tumor-dependent immunogenicity and other factors contributing to tumor response to electrochemotherapy.

5 Conclusions

Tumor response to electrochemotherapy is a complex phenomenon. In this paper, we presented a model that is able to capture the dynamics of two main antitumor effects, namely drug cytotoxicity and immune response. Thus, the model can serve as a tool to quantify the tumor response in terms of direct and immune-mediated cell killing. However, modeling should be considered as a testing hypothesis and thus complementary to experimental work. More profound understanding of immune dynamics would enable to further extend the presented model.

Acknowledgments This work was supported by the Slovenian Research Agency (ARRS) and conducted within the scope of Electroporation in Biology and Medicine (EBAM) European Associated Laboratory (LEA) and the COST Action TD1104 (in particular by a short-term scientific mission COST-STSM-TD1104-21001). Authors would like to thank Gregor Sersa from Institute of Oncology Ljubljana for providing us with the raw data.

References

1. Adkins I, Fucikova J, Garg AD, Agostinis P, Spisek R (2015) Physical modalities inducing immunogenic tumor cell death for cancer immunotherapy. Oncoimmunology 3:e968434
2. Bugaut H , Bruchard M, Berger H, Derangere V, Odoul L, Euvrard R, Ladoire S, Chalmin F, Vegran F, Rebe C, Apetoh L, Ghiringhelli F, Mignot G (2013) Bleomycin exerts ambivalent antitumor immune effect by triggering both immunogenic cell death and proliferation of regulatory T cells. PLoS One 8:e65181
3. Calvet CY, Famin D, Andre FM, Mir LM (2014) Electrochemotherapy with bleomycin induces hallmarks of immunogenic cell death in murine colon cancer cells. Oncoimmunology 3:e28131
4. Cemazar M, Miklavcic D, Sersa G (1998) Intrinsic sensitivity of tumor cells to bleomycin as an indicator of tumor response to electrochemotherapy. Jpn J Cancer Res 89:328–333
5. Cemazar M, Parkins CS, Holder AL, Kranjc S, Chaplin DJ, Sersa G (2001) Cytotoxicity of bioreductive drug tirapazamine is increased by application of electric pulses in SA-1 tumours in mice. Anticancer Res 21:1151–1156
6. Corovic S, Lackovic I, Sustaric P, Sustar T, Rodic T, Miklavcic D (2013) Modeling of electric field distribution in tissues during electroporation. Biomed Eng Online 12:16
7. Domenge C, Orlowski S, Luboinski B, De Baere T, Schwaab G, Belehradek J, Mir LM (1996) Antitumor electrochemotherapy: new advances in the clinical protocol. Cancer 77:956–963
8. Edhemovic I, Brecelj E, Gasljevic G, Marolt Music M, Gorjup V, Mali B, Jarm T, Kos B, Pavliha D, Grcar Kuzmanov B, Cemazar M, Snoj M, Miklavcic D, Gadzijev EM, Sersa G (2014) Intraoperative electrochemotherapy of colorectal liver metastases. J Surg Oncol 110:320–327
9. Gay HA, Taylor QQ, Kiriyama F, Dieck GT, Jenkins T, Walker P, Allison RR, Ubezio P (2013) Modeling of non-small cell lung cancer volume changes during CT-based image guided radiotherapy: patterns observed and clinical implications. Comput Math Methods Med 2013:637181
10. Golden EB, Apetoh L (2015) Radiotherapy and immunogenic cell death. Semin Radiat Oncol 25:11–17
11. Jarm T, Cemazar M, Miklavcic D, Sersa G (2010) Antivascular effects of electrochemotherapy: implications in treatment of bleeding metastases. Expert Rev Anticancer Ther 10:729–746
12. Koch G, Walz A, Lahu G, Schropp J (2009) Modeling of tumor growth and anticancer effects of combination therapy. J Pharmacokinet Pharmacodyn 36:179–197
13. Kotnik T, Kramar P, Pucihar G, Miklavcic D, Tarek M (2012) Cell membrane electroporation- Part 1: The phenomenon. IEEE Electr Insul Mag 28:14–23
14. Kuznetsov V, Makalkin I, Taylor M, Perelson A (1994) Nonlinear dynamics of immunogenic tumors: parameter estimation and global bifurcation analysis. Bull Math Biol 56:295–321
15. Krysko DV, Garg AD, Kaczmarek A, Krysko O, Agostinis P, Vandenabeele P (2012) Immunogenic cell death and DAMPs in cancer therapy. Nat Rev Cancer 12:860–875
16. Markelc B, Bellard E, Sersa G, Pelofy S, Teissie J, Coer A, Golzio M, Cemazar M (2012) In vivo molecular imaging and histological analysis of changes induced by electric pulses used for plasmid DNA electrotransfer to the skin: a study in a dorsal window chamber in mice. J Membr Biol 245:545–554
17. Markelc B, Sersa G, Cemazar M (2013) Differential mechanisms associated with vascular disrupting action of electrochemotherapy: intravital microscopy on the level of single normal and tumor blood vessels. PLoS One 8:e59557
18. Marty M, Sersa G, Garbay JR, Gehl J, Collins CG, Snoj M, Billard V, Geertsen PF, Larkin JO, Miklavcic D, Pavlovic I, Paulin-Kosir SM, Cemazar M, Morsli N, Soden DM, Rudolf Z, Robert C, O'Sullivan GC, Mir LM (2006) Electrochemotherapy—an easy, highly effective and safe treatment of cutaneous and subcutaneous metastases: results of ESOPE (European Standard Operating Procedures of Electrochemotherapy) study. Eur J Cancer Suppl 4:3–13
19. Miklavcic D, Mali B, Kos B, Heller R, Sersa G (2014) Electrochemotherapy: from the drawing board into medical practice. Biomed Eng Online 13:29
20. Miklavcic D, Sersa G, Brecelj E, Gehl J, Soden D, Bianchi G, Ruggieri P, Rossi CR, Campana LG, Jarm T (2012) Electrochemotherapy: technological advancements for efficient electroporation-based treatment of internal tumors. Med Biol Eng Comput 50:1213–1225
21. Miklavcic D, Beravs K, Semrov D, Cemazar M, Demsar F, Sersa G (1998) The importance of electric field distribution for effective in vivo electroporation of tissues. Biophys J 74:2152–2158
22. Mir LM, Orlowski S, Belehradek J, Paoletti C (1991) Electrochemotherapy potentiation of antitumour effect of bleomycin by local electric pulses. Eur J Cancer 27:68–72
23. Mould DR, Walz A-C, Lave T, Gibbs JP, Frame B (2015) Developing exposure/response models for anticancer drug treatment: special considerations. CPT Pharmacomet Syst Pharmacol 4:e00016
24. Pavselj N, Bregar Z, Cukjati D, Batiuskaite D, Mir LM, Miklavcic D (2005) The course of tissue permeabilization studied on a mathematical model of a subcutaneous tumor in small animals. IEEE Trans Biomed Eng 52:1373–1381
25. Rocchetti M, Poggesi I, Germani M, Fiorentini F, Pellizzoni C, Zugnoni P, Pesenti E, Simeoni M, De Nicolao G (2005) A pharmacokinetic-pharmacodynamic model for predicting tumour growth inhibition in mice: a useful tool in oncology drug development. Basic Clin Pharmacol Toxicol 96:265–268

26. Rockne R, Alvord EC, Rockhill JK, Swanson KR (2009) A mathematical model for brain tumor response to radiation therapy. J Math Biol 58:561–578
27. Sersa G, Miklavcic D, Cemazar M, Belehradek J, Jarm T, Mir LM (1997) Electrochemotherapy with CDDP on LPB sarcoma: comparison of the anti-tumor effectiveness in immunocompotent and immunodeficient mice. Bioelectrochem Bioenerg 43:279–283
28. Sersa G, Jarm T, Kotnik T, Coer A, Podkrajsek M, Sentjurc M, Miklavcic D, Kadivec M, Kranjc S, Secerov A, Cemazar M (2008) Vascular disrupting action of electroporation and electrochemotherapy with bleomycin in murine sarcoma. Br J Cancer 98:388–398
29. Sersa G, Teissie J, Cemazar M, Signori E, Kamensek U, Marshall G, Miklavcic D (2015) Electrochemotherapy of tumors as in situ vaccination boosted by immunogene electrotransfer. Cancer Immunol Immunother 64:1315–1327
30. Sersa G, Cemazar M, Miklavcic D (1995) Antitumor effectiveness of electrochemotherapy with cis-diamminedichloroplatinum(II) in mice. Cancer Res 55:3450–3455
31. Sersa G, Miklavcic D, Cemazar M, Rudolf Z, Pucihar G, Snoj M (2008) Electrochemotherapy in treatment of tumours. Eur J Surg Oncol 34:232–240
32. Spratt DE, Gordon Spratt EA, Wu S, DeRosa A, Lee NY, Lacouture ME, Barker CA (2014) Efficacy of skin-directed therapy for cutaneous metastases from advanced cancer: a meta-analysis. J Clin Oncol 32:3144–3155
33. Todorovic V, Sersa G, Flisar K, Cemazar M (2009) Enhanced cytotoxicity of bleomycin and cisplatin after electroporation in murine colorectal carcinoma cells. Radiol Oncol 43:264–273
34. Trdan O, Galmarini CM, Patel K, Tannock IF (2007) Drug resistance and the solid tumor microenvironment. J Natl Cancer Inst 99:1441–1454
35. Zitvogel L, Apetoh L, Ghiringhelli F, Kroemer G (2008) Immunological aspects of cancer chemotherapy. Nat Rev Immunol 8:59–73
36. Zitvogel L, Kepp O, Kroemer G (2011) Immune parameters affecting the efficacy of chemotherapeutic regimens. Nat Rev Clin Oncol 8:151–160

Tadeja Forjanič received a B.S. degree in Physics and a M.S. degree in Medical Physics from the University of Ljubljana in 2011 and 2013, respectively. She is a Ph.D. student in the field of Biomedical Engineering at the University of Ljubljana. Her field of interest is mathematical modeling of biological responses to electroporation-based therapies.

Damijan Miklavčič was born in Ljubljana, Slovenia, in 1963. He received a Masters and a Doctoral degree in Electrical Engineering from University of Ljubljana in 1991 and 1993, respectively. He is currently Professor and the Head of the Laboratory of Biocybernetics at the Faculty of Electrical Engineering, University of Ljubljana. His research areas are biomedical engineering and study of the interaction of electromagnetic fields with biological systems. In the last years, he has focused on the engineering aspects of electroporation as the basis of drug delivery into cells in tumor models in vitro and in vivo. His research includes biological experimentation, numerical modeling and hardware development for electrochemotherapy, irreversible electroporation and gene electrotransfer.